Dimensional modeling of biomass pyrolysis based on a nodal approach

Razvan Vijeu, Luc Gerun, Jerome Bellettre, Mohand Tazerout, Cathy Castelain

DIMENSIONAL MODELING OF BIOMASS PYROLYSIS BASED ON A NODAL APPROACH

Rãzvan Vîjeu, Luc Gerun, Jérôme Bellettre*, Mohand Tazerout
Ecole des Mines de Nantes, DSEE, 4
rue Alfred Kastler, B.P. 20722, 44 307 NANTES Cedex 3, France
Cathy Castelain
Laboratoire de Thermocinétique de l'Université de Nantes UMR CNRS 6607
rue Christian Pauc, BP 50609, 44306 NANTES Cedex 3, France

ABSTRACT

The purpose of the present research is to develop a numerical model for the biomass gasification processes suitable for the dimensioning of industrial installation. The end use of the producer gas being often internal combustion engines systems, the model concentrates on the quantitative and qualitative aspects of the process, with a particular interest in the problem of tar formation and destruction. This study focuses on the first two steps of the process: drying and pyrolysis. The pyrolysis model presented in this paper consists in a coupling between a heat transfer model based on a nodal approach and a chemical model for the thermal decomposition of the pyrolysed material. Drying is considered as a sub process included in pyrolysis. The shown results are in good agreement with experimental data.

Keywords: pyrolysis, nodal modeling, biomass

NOMENCLATURE

C_p	specific heat [J/kg/K]
k	reaction constants [s^{-1}]
K	permeability [m^2]
m	mass [kg]
$\dot{m}$	mass flow [$kg/m^3/s$]
p	pressure [Pa]
S	surface [m^2]
t	time [s]
T	temperature [K]
u	velocity [m/s]
V_c	control volume [m^3]
x	distance [m]

Greek letters

ρ_s	apparent density [kg/m^3]
ε	bed void fraction
Φ	heat flux [W]
μ	fluid viscosity [kg/m/s]

Subscripts

C	char
g, G	gas
s	solid
T	tar
W	wood
v	vaporization

INTRODUCTION

As a result of the present environmental context more and more attention is given to the biomass conversion technologies as green energy sources. This fact accents the need for accurate models that can predict thermal decomposition behavior and that can assist the scale up of new types of installations [1].

This work aims to investigate the opportunity of implementing a new type of model that can provide fast but accurate information regarding the thermal decomposition of biomass. Usually the phases of a gasification process are drying, pyrolysis and oxidation/reduction. Only drying and pyrolysis phases are modeled in this paper.

*Corresponding author. Phone +33 (0) 2 51 85 82 96
Fax: +33 (0) 2 51 85 82 99, E-mail: jerome.bellettre@emn.fr

The proposed model combines a nodal numerical method, often employed for heat transfer cases, with a chemical mechanism for the thermal decomposition and with a simplified mass transfer model. The unsteady state model can predict the parameters of the pyrolysis process depending on the material properties and the chosen chemical sub-model. The model also allows the study of the influence of different reactor geometry on the global process and offers the scale up possibility.

REACTOR GEOMETRIES

As stated earlier, the model should be able to study the influence of the reactor geometry on the overall pyrolysis process. However, it is generally admitted that the geometry of the reactor can only significantly influence its heat transfer capabilities, such as surface to volume ratio for example. Since the non-oxidative pyrolysis is a mainly endothermic process it is highly dependent on the temperature, thus dependent of the amount of heat introduced into the reactor through the walls. From this point of view the advantage lies with the geometry that provides a bigger heat-exchanging surface for a constant volume.

The symmetrical geometry is also preferred because it is more representative for the actual industrial installations. The present study is conducted on a cylindrical reactor.

NUMERICAL ALGORITHM

The nodal method is widely used for heat transfer modelling of non-homogenous media in steady or unsteady state. It allows the construction of simple heat transfer models by linking interacting elements and is more adequate for this type of problems comparing to the finite volumes or finite element methods. The principles of this numerical method are discussed in [2], [3] and [4].

For better understanding all the concepts of the nodal method will be exemplified on the reaction volume presented in Figure 1. It is filled with spherical biomass particles with the same diameter forming a porous bed. If the bed is considered homogenous and isotropic, an annular discretization like the one shown in Figure 1 can be applied. If each annular element is concentrated in a node, the result is a two dimensional nodal grid. However, if the zone is not homogenous and isotropic, a more complex discretization pattern has to be employed, by inserting several separation planes passing through the axis of the cylinder.

The nodal numerical method concentrates the entire control volume is into a single point in the center of the volume, the temperature being assumed uniform within the volume.

For the annular shaped volumes the resulting nodal grid is presented in Figure 2. It represents a half-axial cross section of the cylinder, as it is discretized in Figure 1. The distance between the nodes usually varies from a few millimeters to a few centimeters. The filled points correspond to the reaction volume while the unfilled points represent the boundaries. The interactions between a boundary point and a reaction point are defined separately due to the particularity of various phenomenons in their vicinity.

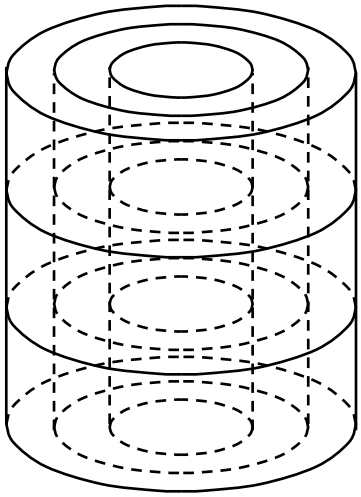

Figure 1. Reactor geometry and discretization

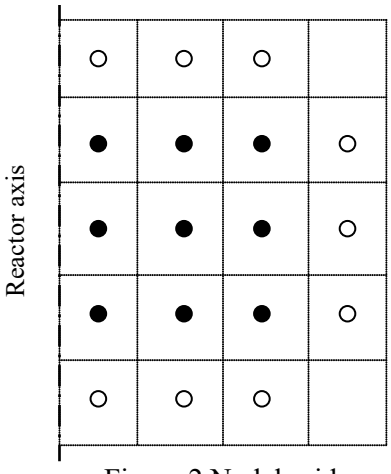

Figure 2.Nodal grid

The algorithm of the nodal method implies that the value of a certain parameter at the current time step is calculated using the available data from the previous time step. This explicit technique allows analytical solving of differential equations

considering that certain parameters remain constant during the imposed time period. This simplification eliminates the need of iterating or solving complex systems of equations and provides a fast calculation method with minimal precision loss.

HEAT TRANSFER SUB MODEL

The heat transfer modeling of the porous bed during pyrolysis is based on the previous work presented in [5]. A number of assumptions are made in order to simplify the model. Depending of the heating configuration and the gas flow in the reactor, a choice has to be made regarding the temperature field of the solid and fluid phases. The thermal equilibrium between the two phases is best suitable if the cylinder in Figure 1 is heated only on the lateral side for example, with the gases escaping through the topside. However, if the same cylinder is also heated on the bottom side, the hot gas formed in the lower layers must pass through the cooler superior layers. In this case the thermal equilibrium is no longer suitable and two temperature fields need to be employed for a better description of the heat transfer phenomenons. In this work, the latter case is retained and two temperature fields are defined.
Heat transfer within the fluid can also be simplified by assuming that the fluid phase exchanges heat only by convection with the solid phase, thus neglecting its own conduction and radiation. The solid phase radiation and conduction can be quantified together in a parallel mechanism.
The heat transfer equation applicable to the nodal model is given by [2] for a node *i* surrounded by *j* other nodes:

$$m_i C_{pi} \frac{dT_i}{dt} = \sum_j \Phi_{ij} + \sum_k \Phi_{ki} \qquad (1)$$

The term Φ_{ij} represents the flux exchanged between the nodes *i* and *j* and is expressed by equation (2).

$$\Phi_{ij} = G_{ij} \cdot (T_i - T_j) \qquad (2)$$

The G_{ij} factor is the conductance between the two nodes and it is calculated in relation to the material properties and the reactor geometry. The Φ_{ki} flux represents the source term for the node *i* and it is a function of the heat of reaction presented in table 1 and the kinetic constants of the chemical process. If two temperature profiles are to be taken into account, the equation (1) can be applied for each phase and the heat flux resulted form the convection between the two phases can be included as heat source terms.

CHEMISTRY OF DRYING AND PYROLYSIS

Drying is the first heat driven process that occurs during the global gasification process. Evaporation of the moisture content of the biomass requires a significant amount of heat, thus drying must be included in the model.
Bryden et al. [10] and Peters et al.[11] present two models for drying of wood packed beds. The first model is considering the vaporization process as a simple heterogeneous reaction with the rate described by an Arrhenius expression. Bryden [10] proposes rate parameters of $A_v = 5.13 \times 10^{10}$ s^{-1} and $E_v = 88$ kJ/mol. This mechanism is proven to be numerically stable but the kinetic parameters presented above may be difficult to use in situations different of those in which the data has been calculated.
To overcome this disadvantage a second drying mechanism is put in place: the amount of heat available at a temperature greater than the evaporation temperature is consumed by the drying process. This requires the use of a Dirac function.

One of the advantages of the nodal method is its versatility in the use of various chemical mechanisms. The kinetic models are best suitable for the nodal method but combinations between such models and equilibrium models are possible.
Different kinetic models are presented in [7], [8] and [9]. The model presented by Mousques [9] and Bryden [10] (Figure 3) is chosen to exemplify the use of kinetic mechanisms.

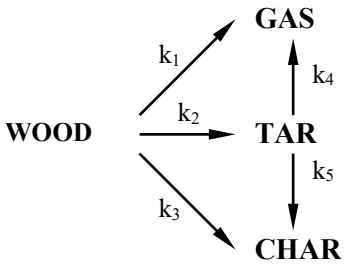

Figure 3: Chemical model

The wood is decomposed by three simultaneous primary reactions producing a solid carbonaceous residue (the char), a pseudo species of condensable

gases (the tar) and a pseudo species of non-condensable gases (the gas). The secondary decomposition of the tar produces more gas and char. The reaction constants obey the Arrhenius formalism and the kinetic data is presented in Table 1.

Table 1: Kinetic data for the chemical model [10]

Reaction	A_i (s^{-1})	E_{ai} (J/mol)	ΔH_i (J/kg)
1	$1.43\ 10^4$	$8.86\ 10^4$	$4.18\ 10^5$
2	$4.13\ 10^6$	$1.127\ 10^5$	$4.18\ 10^5$
3	$7.38\ 10^5$	$1.065\ 10^5$	$4.18\ 10^5$
4	$4.28\ 10^6$	$1.08\ 10^5$	$-4.2\ 10^4$
5	10^5	$1.08\ 10^5$	$-4.2\ 10^4$

For this chemical model all the reactions are first order decompositions. The parameters used for the expressions of the kinetic laws are given by equations (3) and (4).

$$\rho_s = \frac{m_s}{V_c} \tag{3}$$

$$\rho_g = \frac{m_g}{\varepsilon \cdot V_c} \tag{4}$$

The two parameters represent the apparent densities of the solid or gaseous pseudo species. In the case of solids, the density is relative to a control volume V_c. while for gases it is relative to the void volume available in the same control volume.
The mass balance for the four pseudo-species involved in the pyrolysis process is given by equations (4) to (7).

$$\frac{d\rho_W}{dt} = -(k_1 + k_2 + k_3)\rho_W \tag{5}$$

$$\frac{d\rho_C}{dt} = k_3 \cdot \rho_W + k_5 \cdot \rho_T \tag{6}$$

$$\frac{d\rho_G}{dt} = k_1 \cdot \rho_W + k_4 \cdot \rho_T \tag{7}$$

$$\frac{d\rho_T}{dt} = k_2 \cdot \rho_W - (k_4 + k_5) \cdot \rho_T \tag{8}$$

The heats of different reactions in Table 1 provide means of calculating Φ_{ki} from equation (1).
The versatility of this approach lies in the fact that for a different material, characterized by different reaction mechanism, the equations (5) to (8) are easily replaceable with those resulted from the new mechanism. However, the mass balance for the fluid phase for each control volume must include the terms describing the flow of the gasses in the reactor.

MASS TRANSFER SUB MODEL

If the heat transfer and the chemistry are easily integrated with the nodal method concepts, the fluid flow component represents the difficulty of this method, mainly due to the transitory nature of the global process.
The first approximation to be made is to consider all the gasses as ideal. This allows the evaluation of the pressure build up in each grid node during the imposed time step. The fluid velocities can be obtained knowing the pressures in each node and using Darcy law for porous media:

$$u = -\frac{K}{\mu}\frac{\delta p}{\delta x} \tag{9}$$

Patankar [6] recommends defining a secondary grid. This new grid will have as nodes the interfaces between the adjacent cells and the velocities will be disposed as shown in Figure 4. Since the pressure data is available in discrete positions, the equation (9) has to be slightly modified. Equation (10) represents a more suitable form of the Darcy law.

$$u = -\frac{K}{\mu}\frac{\Delta p}{\Delta x} \tag{10}$$

The term Δp represents the pressure difference between two neighbor nodes and Δx represents the distance between the nodes.

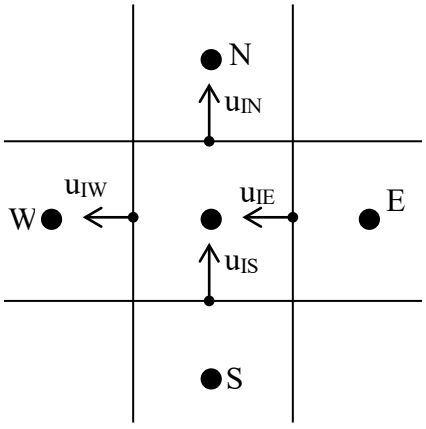

Figure 4: The velocity grid

The mass transfer between two nodes can be evaluated using the calculated velocity and the common surface of the two nodes.

$$\dot{m} = uS\rho_g \quad (11)$$

Besides the convective mass transfer, a diffusional mass transfer component can also be defined using a transfer coefficient. In this model there is no need to account for this kind of mass transfer.
However, a mass transfer model based on the Darcy law is difficult to use in combination with the nodal discretization technique. The problem consists in the fact that the gas flow phenomenon has a very small time constant compared to the heat transfer and the chemistry time constants. This problem causes unacceptable simulation delays and for this reason the mass transfer mechanism must be implemented by separating the mass flow phenomenon of the rest of the processes. For this reason a simpler model is required. The new mass transfer sub model is based on two essential assumptions:
- fluid cannot flow downwards;
- all fluid produced during a time step by the chemical sub model leaves the reactor in the same time step (at the end of each time step the pressure in the reactor is 1 bar).
The mass transfer algorithm consists in finding a point of maximum pressure in each radial layer. From this point the fluid can flow upwards and sideways. To the left of this point the fluid will only go upwards and to the left, while to the right of the maximal pressure point the fluid will flow only upwards and to the right. This algorithm is applied to all the radial layers of the reactor, starting with the bottom one. In a layer, the mass balance is calculated for each node starting with the maximal pressure point.
The amount of fluid transported upward and sideways can be evaluated either by considering them proportional with the pressure drop on the corresponding direction or by imposing a fixed percentage of the fluid that will go sideways. In this work a fixed percent choice is made.

COUPLING OF SUB MODELS

As stated before, the pyrolysis model links three sub models describing three different phenomenons. Some difficulties can arise in deciding the order in which the sub models are to be applied. The logical chain of events is:

1. heat transfer determines the advancement of the chemical reactions;
2. chemical reactions caused by the transferred heat determine a rise of pressure in the nodes;
3. flow of gas produced by the chemical reactions causes a redistribution of the gaseous reactants and determines a new convective heat transfer component between gas and solid.

The first step of the calculation chain can be either one of the three events, but their order should be respected since it represents the causal chain of the process.

EXPERIMENTAL INSTALLATION

The experimental installation consists in a cylindrical steel reactor placed in an insulated heater, as shown in Figure 5. The reactor is 255 mm high, has a diameter of 166 mm and the wall is 2 mm thick. The heater can provide 15 kW of power and is regulated by a PID regulator that uses a type N thermocouple (T_1). The measurement points T_2 and T_4 also use type N thermocouples. The distance from the bottom is 10 mm. T_2 is placed at 10 mm from the reactor wall while T_4 is placed at 5 mm from it's center.

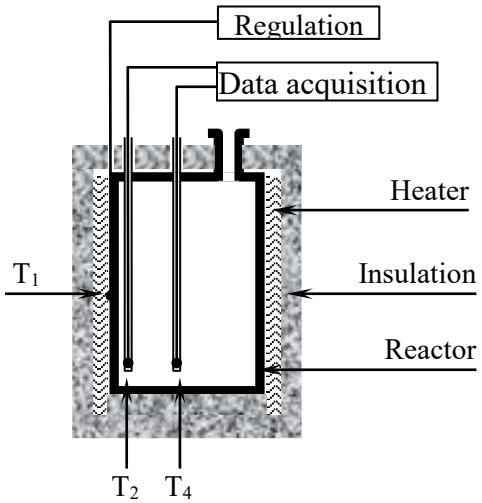

Figure 5: Experimental unit

The biomass used in the experiments is oak sawdust with particle diameter between 0.8 mm and 0.9 mm. The equivalent formula is $CH_{1.51}O_{0.81}N_{0.0046}$ and the water content is 15% wb.

RESULTS

The presented results are simulated using the simplified mass transfer sub model. The percentage of fluid flowing sideways is set at 10%. The most influenced parameters by this choice of

mass transfer are the apparent densities of the two fluid pseudo-species [2].

Figure 6 shows a comparison between the experimental data and simulated data for the solid temperatures T_2 and T_4.

The simulation is made for a 1 mm vertical and horizontal distance between nodes and for a time step of 0.1 seconds.

The heating rate of the reactor is set at 12 °C per minute. Reactor temperature rises until it reaches 600°C where is remains constant.

The characteristics of the material are those presented in the previous section.

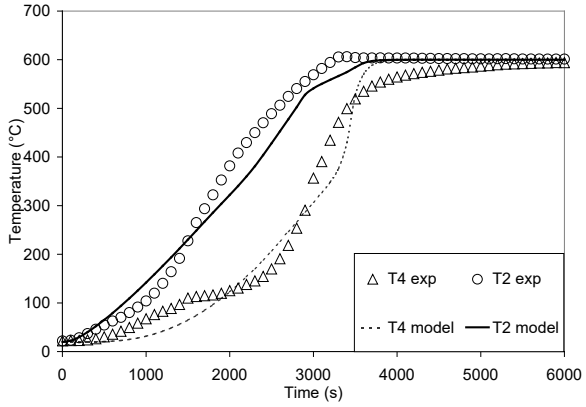

Figure 6. Experimental and simulation data

The pyrolysis front is similar to the one shown in Figure 8, although it is calculated for a different reactor configuration.

The reaction front reaches the center of the reactor after approximately 4000 seconds consuming the remaining unreacted wood. The predicted time for the completion of pyrolysis agrees well with the experimental time.

SENSIBILITY TESTS

The results of the model can be sensitive to the discretization degree of the reactor and to the time step of the simulation.

The sensibility study is conducted on a different configuration from the experimental one described in the previous section.

The reactor is similar to the real one but it has a height of 30 cm and a radius of 7 cm. The main grid has 300 vertical nodes and 70 horizontal nodes, thus a nodal distance of 1 mm in both directions. The sides of the reactor are heated at 800 K and the time step is 0.1 seconds.

Figure 7 and Figure 8 present the temperature profile and the wood apparent density profile inside this reactor after 1200 real seconds of simulation in the configuration used for the sensibility tests.

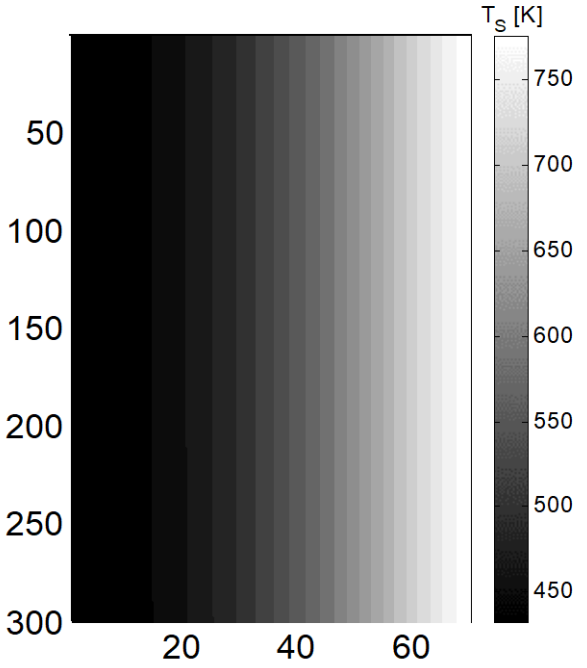

Figure 7: Solid temperature field (t=1200s)

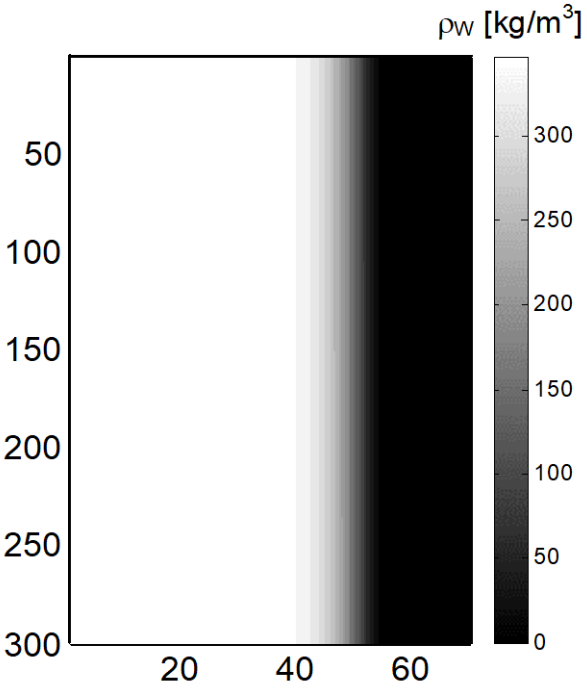

Figure 8: Wood apparent density field (t=1200s)

Time step sensibility

Time step sensibility tests are made on a spatial discretization of 5 mm between nodes and for three different time steps. The simulation is halted

after 1200 real seconds in order to compare the solid temperature and the wood apparent density for the three time steps.

Figure 9 shows the three profiles for the solid temperature calculated at a time step between 0.1 and 1 second and at a radial section situated at 150 mm from the top of the reactor. Figure 10 shows the three profiles for the wood apparent density for the same three time steps and for the same radial section.

Figures 9 and 10 show that the model is not very sensitive to the simulation time step. However, it seems that a larger distance between the nodes produces an increased sensibility to the time step (results not shown here).

In the case of the chemical data the differences are slightly more important due to a high sensibility of the kinetic constants to the temperature variations.

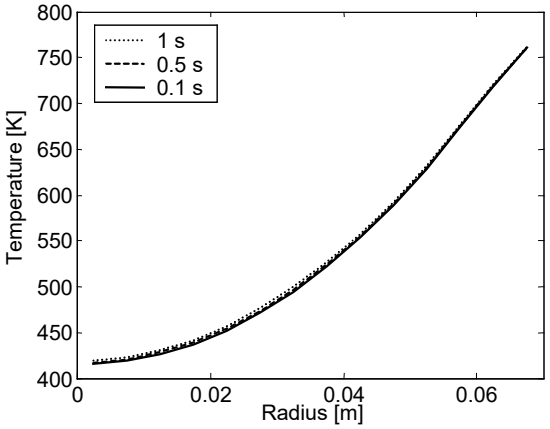

Figure 9: Solid temperature (t=1200s) (300x70 nodes)

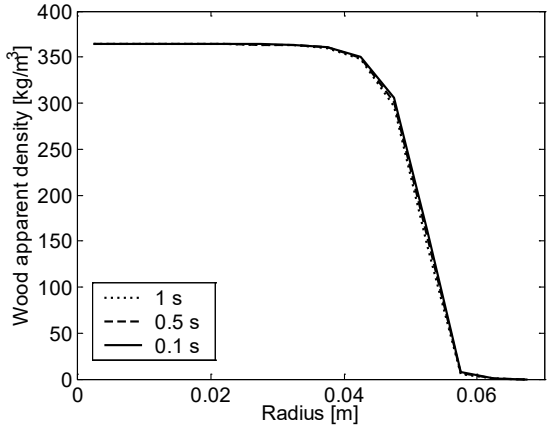

Figure 10: Wood apparent density (t=1200s) (300x70 nodes)

Meshing sensibility

The tests for the grid spacing sensibility are made on the same reactor configuration, for a time step of 0.1 s and for a discretization of 10 mm, 5 mm and 1 mm. The retained data is presented in Figures 11 and 12.

The study shows that the nodal distance significantly influences the results. The big differences suggest that not even a distance of 5 mm between the nodes is sufficiently small for an accurate result. A smaller distance also provides an improved resolution especially in the proximity of the boundaries.

Figure 11 shows the solid temperature profiles in a section situated at 150 mm from the top of the reactor. In this case the differences are important but the profiles are similar, regardless of the discretization.

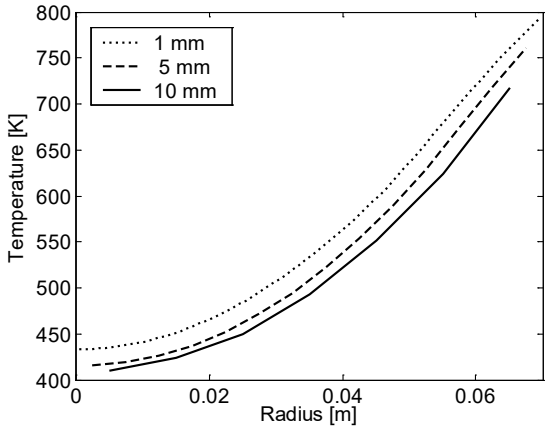

Figure 11: Solid temperature (t=1200s, dt=0.1s) (300x70 nodes)

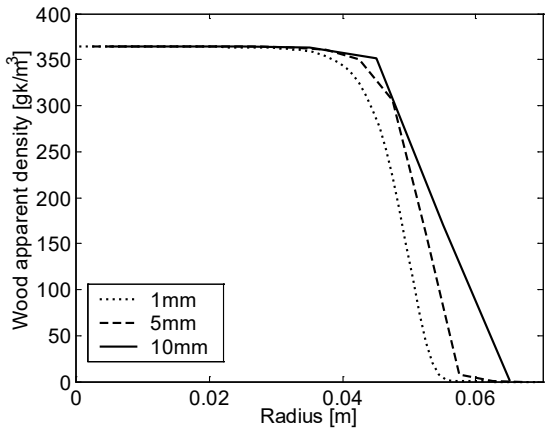

Figure 12 Wood apparent density profiles (t=1200s, dt=0.1s) (300x70 nodes)

The chemical data in Figure 12 seems to be more sensible to the grid spacing. The wood apparent density shows a pronounced sensibility zone only on the reaction front.
The comparisons in Figures 11 and 12 for the three different grid spacing show that from this point of view a distance between node greater than 1 mm produces results highly inaccurate and unacceptable. Even so, the study should be continued for even smaller distances in order to test the accuracy of the 1 mm set of data.
The overall sensibility study shows the importance of choosing an adequate nodal grid and time step. Even if in this case the results do not impose a very small time step, from our experience, a smaller distance between nodes also requires a smaller time step.

CONCLUSION

This work presents a nodal model of the pyrolysis process, as a link between a heat transfer model, a chemical model and a simplified mass transfer model. The concepts of the method are shown and the results are compared with experimental data. From a thermal point of view the simulated results are in good agreement with experimental data.
A sensibility study is also conducted in order to describe the behavior of the model to the variation of spatial discretization and of imposed time step.
As a perspective, the mass transfer model can be improved to take into account the actual pressure field in the reactor. The model could also be modified to simulate continuous processes.

REFERENCES

[1] Di Blasi C., *Dynamic behaviour of stratified downdraft gasifiers*, Chemical Engineering Science 55 (2000) 2931 – 2944

[2] Saulnier J.-B., Alexandre A. *La modélisation thermique par la méthode nodale, ses succès et ses limites* Revue Generale de Thermique 1985; 280 : 363 - 372

[3] Lagnotte P., Bertin Y., Saulnier J.-B. *Analyse de la qualité de modèles nodaux réduits à l'aide de la méthode des quadripôles*. International Journal of Thermal Sciences 1999; 38 : 51 – 65

[4] Belletre J., Sartre V., Biaist F., Lallemand A. *Transient state study of electric motor heating and phase change solid-liquid cooling.* Applied Thermal Engineering 1997; 17: 17-31

[5] Vijeu R. A., Tazerout M. *Modélisation et dimensionnement d'une zone de pyrolyse d'un gazogène co-courant.* In: Proceedings of COFRET'04, Nancy, 2004

[6] Patankar S.V. *Numerical heat transfer and fluid flow.* USA: Taylor & Francis, 1980

[7] Chen G., Andries J., Spliethoff H, Fang M. *Kinetics of biomass wastes pyrolysis for fuel gas production*. In: Proceedings of ECOS 2002

[8] Babu B. V., Chaurasia A. S. *Pyrolysis of biomass: improved models for simultaneous kinetics and transport of heat, mass and momentum* Energy Conversion and Managemnt 2004; 45: 1297-1327

[9] Mousques M. *Modélisation du couplage réactions chimiques – transferts de chaleur/matière en vue du dimensionnement des réacteurs de pyrolyse* Ph. D. report, Université de Perpignan, 2001

[10] Bryden K.M., Ragland K.W., Rutland C.J.*Modeling thermally thick pyrolysis of wood* Biomass and Bioenergy 2002 ; 22 :14-53

[11] Peters B., Bruch C., *Drying and pyrolysis of wood particles : experiments ans simulation* J. Anal. Appl. Pyrolysis 2003 ; 70 :223-250

[12] Vijeu R.A., Bellettre J., Tazerout M., *Nodal modeling of biomass thermochemical decomposition* In Proceedings of SIMS 04, Copenhagen, September 2004, p. 129-135